Geochemistry, Geophysics, Geosystems

RESEARCH ARTICLE
10.1029/2020GC009180

Juvenile Eastern Oysters More Resilient to Extreme Ocean Acidification than Their Mud Crab Predators

L. F. Dodd[1], J. H. Grabowski[3], M. F. Piehler[1], I. Westfield[2,3], and Justin B. Ries[2,3]

[1]Institute of Marine Science, University of North Carolina at Chapel Hill, Morehead City, NC, USA, [2]Department of Marine Sciences, University of North Carolina at Chapel Hill, Chapel Hill, NC, USA, [3]Northeastern University, Nahant, MA, USA

Key Points:

- Juvenile eastern oysters maintained net-positive calcification rates even in seawater undersaturated with respect to calcite
- Despite a net-positive calcification rate, oyster shells showed dissolution and delamination in seawater undersaturated with respect to calcite
- Mud crabs were not able to maintain the same net-positive calcification rates as their oyster prey in the high acidification treatment

Correspondence to:
L. Dodd,
lukefdodd@gmail.com

Citation:
Dodd, L. F., Grabowski, J. H., Piehler, M. F., Westfield, I., & Ries, J. B. (2021). Juvenile eastern oysters more resilient to extreme ocean acidification than their mud crab predators. *Geochemistry, Geophysics, Geosystems*, *22*, e2020GC009180. https://doi.org/10.1029/2020GC009180

Received 14 MAY 2020
Accepted 20 NOV 2020

Abstract Ocean acidification is predicted to impair marine calcifiers' abilities to produce shells and skeletons. We conducted laboratory experiments investigating the impacts of CO_2-induced ocean acidification (pCO_2 = 478–519, 734–835, 8,980–9,567; $\Omega_{calcite}$ = 7.3–5.7, 5.6–4.3, 0.6–0.7) on calcification rates of two estuarine calcifiers involved in a classic predator-prey model system: adult *Panopeus herbstii* (Atlantic mud crab) and juvenile *Crassostrea virginica* (eastern oyster). Both oyster and crab calcification rates significantly decreased at the highest pCO_2 level. Notably, however, oysters maintained positive net calcification rates in the highest pCO_2 treatment that was undersaturated with respect to calcite, while mud crabs exhibited net dissolution (i.e., net loss of shell mass) in calcite-undersaturated conditions. Secondary electron imaging of oyster shells revealed minor microstructural alterations in the moderate-pCO_2 treatment, and major microstructural and macrostructural changes (including shell dissolution, delamination of periostracum) in the high-pCO_2 treatment. These results underscore the threat that ocean acidification poses for marine organisms that produce calcium carbonate shells, illustrate the strong biological control that some marine calcifiers exert over their shell-building process, and shows that ocean acidification differentially impacts the crab and oyster species involved in this classical predator-prey model system.

1. Introduction

Anthropogenic carbon dioxide (CO_2) emissions have already reduced ocean surface pH by nearly 0.1 since 1900 and are projected to acidify surface seawater by an additional 0.1–0.4 units by 2100 (Brewer, 1997; Hoegh-Guldberg et al., 2014). This projected decrease in seawater pH could nearly halve the carbonate ion concentration and calcium carbonate saturation state of seawater (Brewer, 1997), making it more difficult for calcifying marine organisms to build, maintain, and repair their protective shells and skeletons. These effects may be particularly deleterious for marine calcifiers inhabiting regions with naturally low calcium carbonate saturation states, such as estuaries (Waldbusser et al., 2011), environments near or below the carbonate compensation depth, and high-latitude seas that are more soluble with respect to CO_2 because of their lower temperatures (Fabry et al., 2009).

The effects of CO_2-induced ocean acidification on marine organisms that utilize $CaCO_3$ have received increased attention over the last decade, with laboratory experiments and field studies revealing that calcification responses to CO_2-induced ocean acidification vary widely across taxa (Azevedo et al., 2015; Gattuso et al., 1998; Harvey et al., 2013; Hendriks et al., 2010; Kroeker et al., 2010; Langdon et al., 2000; Langdon, 2005; Ries et al., 2009). This variation in calcification responses to ocean acidification may be attributable to a range of factors, including the presence and extent of protective organic layers, regulation of protons at the calcification site, utilization of photosynthesis that is potentially fertilized by elevated pCO_2, and the relative solubility of their skeletal mineral polymorphs (Ries et al., 2009). Owing to the variety of potential factors affecting how marine calcifiers will respond to ocean acidification, empirical studies are needed to assess species-specific responses to predicted future CO_2-induced ocean acidification. Here, we present the results of controlled laboratory experiments conducted to investigate the impact of ocean acidification on the calcification rates of two species of estuarine marine calcifiers: the ecologically, economically, and culturally important foundation species, the eastern oyster (*Crassostrea virginica*), and the Atlantic mud crab (*Panopeus herbstii*), a major predator of juvenile eastern oysters.

The Atlantic mud crab and eastern oyster are abundant estuarine species in the eastern and gulf coasts of the United States. Owing to its ability to build reefs and filter large volumes of water, the eastern oyster is an important ecosystem engineer in estuarine systems. Atlantic mud crabs are a major predator of eastern oysters during the oyster's juvenile life stage (Menzel & Nichy, 1958; Meyer, 1994) and may be the dominant crustacean predator of oysters in systems where they co-exist (Rindone & Eggleston, 2011). Eastern oysters and mud crabs may be more vulnerable to the effects of ocean acidification than open-ocean species owing to the relatively low salinity, high inputs of organic and inorganic carbon and nutrients, and low carbonate ion concentration of their estuarine habitat-factors that may amplify the negative impact of rising atmospheric pCO_2 on the calcium carbonate saturation state of seawater (Waldbusser et al., 2011).

Postlarval eastern oysters primarily form shells from the relatively stable low magnesium calcite form of calcium carbonate, although small portions of the shell are composed of the more soluble high-magnesium calcite form (Carriker et al., 1991; Korringa, 1951; MacDonald et al., 2010; Taylor & Layman, 1972). Moreover, the relatively high surface area of the eastern oyster's shell renders it particularly vulnerable to dissolution in high-CO_2 conditions (Ries et al., 2016). This vulnerability may be exacerbated by the oyster's patchily distributed periostracum, which may confer less protection to their shell than the periostraca of other bivalves that possess more hydrophobic and continuous periostraca, such as clams and mussels (Ries et al., 2009). Eastern oysters also maintain their extrapallial fluid—their putative calcifying fluid—at lower pH than the surrounding seawater (Crenshaw, 1972; Crenshaw & Neff, 1969; Downey-Wall et al., 2020; Liu et al., 2020; Sutton et al., 2018), which may also increase their vulnerability to CO_2-induced ocean acidification (Ries, 2011).

In the absence of secondary stressors (salinity, temperature), the net rate of calcification (i.e., gross calcification minus gross dissolution) of postsettlement oysters typically declines relatively linearly with decreasing calcite saturation states (Ω_C). However, single and multistressor environments experiments have shown that oysters can continue producing new shell material even under Ω_C as low as 0.7 (i.e., conditions favoring dissolution of abiogenic calcite; Beniash et al., 2010; Ries et al., 2009; Waldbusser et al., 2011). Increased pCO_2 also decreases shell strength and soft tissue mass, causes changes in shell microstructure (Beniash et al., 2010), and either has no effect on (Matoo et al., 2013) or causes an increase in basal metabolism (Beniash et al., 2010) of the eastern oyster. Other oyster species have responded similarly to acidification. Postsettlement Pacific oysters (*Crassostrea gigas*) and Sydney rock oysters (*Saccostrea glomerata*) generally exhibit strong negative linear responses in net calcification to acidified conditions (Gazeau et al., 2007; Parker et al., 2010). However, at least one study found that calcification rates of recently settled Pacific oysters increased at $\Omega_C = 0.66$ ($pCO_2 = 2{,}874$ μatm) relative to individuals grown under control conditions ($pCO_2 = 524$ μatm; $\Omega_C = 2.70$), with no significant difference in ultrastructure relative to control specimens (Ginger et al., 2013). Although oysters are generally negatively impacted by ocean acidification, uncertainty remains over the degree to which vulnerability varies by species, across specific life stages, and as a function of environmental conditions and exposure histories.

Less is known about the response of Atlantic mud crabs to CO_2-induced ocean acidification and prior ocean acidification studies on decapod crustacea have yielded mixed results. For example, Ries et al. (2009) found that adults of three species of decapod crustacea, including the eastern king prawn (*Penaeus plebejus*), American lobster (*Homarus americanus*), and blue crab (*Callinectes sapidus*), exhibited an increase in calcification rate with decreasing pH for values as low as 7.31 ($\Omega_{C=}$ 0.7). In contrast, the calcification rates of juvenile Tanner crabs (*Chionoecetes bairdi*) decreased under elevated pCO_2 ($pCO_2 = 792$ μatm; $\Omega_C = 1.38$) relative to the control ($pCO_2 = 438$ μatm; $\Omega_C = 2.27$), and calcification rate of the juvenile red king crab (*Paralithodes camtschaticus*) was unaffected by a similar degree of acidification (Long et al., 2013).

Decapod crustacea typically produce their carapaces from high-magnesium calcite (5–12 mol % $MgCO_3$) and create a hydrophobic epicuticle that minimizes contact between seawater and mineralized portions of the carapace (Chave, 1954; Plotnick et al., 1988; Ries et al., 2009). A prior study investigating ion flux at the shell boundary of blue crabs (*C. sapidus*) suggests that this species elevates pH and, thus, calcite saturation state at the site of calcification in support of shell mineralization (Cameron, 1989), although a recent study investigating boron isotopes in the shells of blue crabs suggests that this species exerts little control over its calcifying fluid pH (Liu et al., 2020). Regardless of the exact reason(s), controlled ocean acidification experiments show that decapod crustacea exhibit variable responses to CO_2-induced ocean acidification (e.g.,

Long et al., 2013; Ries et al., 2009). Additional studies are needed to determine the cause of this variability, which should inform predictions of how these economically and ecologically important taxa will respond to future ocean acidification.

To investigate the impact of CO_2-induced ocean acidification on shell production by two ecologically important estuarine species in the eastern US, specimens of adult Atlantic mud crabs and juvenile eastern oysters were grown for 10 weeks under three calcite saturation states (Ω_C = 7.3–5.7, 5.6–4.3, 0.7–0.6). These levels corresponded to present-day and predicted future pCO_2 scenarios, including an undersaturated treatment in which raw (i.e., noninhabited) oyster shell was previously shown to rapidly dissolve (Ries et al., 2016).

2. Materials and Methods

Methods detailing growth conditions, measurement, and calculation of carbonate system parameters, and quantification of calcification rates via buoyant weighing are described in detail in a related study (Dodd et al., 2015) and summarized below. This study is part of a set of experiments designed to investigate the effect of variable calcification rates on a predator-prey relationship under ocean acidification. The design includes treatments to test for an effect of prey defenses induced by exposure to predator cues (e.g., increased calcification by prey) (Newell et al., 2007). However, a number of methodological decisions severely limited the likelihood of observing a change in oyster calcification due to an induced defense response. Some methodological choices were made in order not to bias the behavioral aspect of the study, which were published separately (Dodd et al., 2015), while others were made without the benefit of forthcoming research (present study conducted in 2011; Johnson & Smee, 2012; Robinson et al., 2014). These treatments remain in the dataset and are a fully analyzed component of the results. However, due to the drawbacks of this experimental design, discussion of these results is restricted to reflection on the design itself.

2.1. Culture Conditions

Hatchery-raised juvenile wild-strain eastern oysters (*C. virginica*; 18.7 ± 3.8 mm shell height; obtained from Jonny Oyster Seed of St. Leonard, Maryland) and wild-caught adult Atlantic mud crabs (*P. herbstii*; 24.8 ± 1.6 mm carapace width; obtained from intertidal oyster reefs near Morehead City, North Carolina) were raised for 71 days in 34-L glass aquaria containing seawater formulated at pCO_2 (SE) of 499 (14), 785 (19), and 9,274 (276) μatm (Table 1). Oysters (30 per tank) were raised in an orthogonal 3 × 2 design with the three acidification levels described above and two crab cue levels (predators present or absent), while crabs were raised in a 3 × 1 design with the same three acidification levels. Crabs (seven per replicate aquarium) were isolated in chambers throughout the experiment to control individual feeding rates and prevent cannibalism, while allowing for seawater and cue circulation. All treatment conditions were replicated threefold. Prior to the start of the experiment, oysters were maintained in a ca. 500-L tank for no more than 7 days in conditions mirroring the experimental tanks without the addition of CO_2-enriched air, while crabs were placed directly into experimental tanks following collection and processing. All organisms were placed into experimental tanks containing experimental seawater with unmodified carbonate chemistry, immediately before CO_2 treatments began. CO_2 conditions stabilized within 36 h.

Seawater within each tank was continuously filtered (757 L h^{-1}) with a hanging power filter that contained a nylon-floss activated-carbon filter. Circulation of seawater within each tank was enhanced with a 400 L h^{-1} powerhead. Each tank was covered with a transparent 3-mm plexiglass sheet with both tank and attached filtration system wrapped with cellophane to promote equilibration between the gas mixtures and the experimental seawaters and to minimize evaporative water loss. Seventy-five percent seawater changes were performed weekly. Seawater samples were obtained midway between water changes to acquire average values for water chemistry parameters in the treatment tanks. Tanks were illuminated for 12 h per day with standard white fluorescent lights (32 Watts, T8 6,500 K) to simulate oysters' and crabs' natural light cycle. Every 2 days, oysters were fed 14 mL (approximately 0.06 g dry weight; Espinosa & Allam, 2006) per tank of a commercial blend of algae (*DT's Live Marine Phytoplankton*, Sycamore, IL, USA) and each crab was provided 50 ± 7 mg dry weight of frozen *Artemia* sp. by eyedropper into their individual containment chamber.

Table 1
Average Calculated Parameters [pCO_2 of Gas in Equilibrium With Seawater ($pCO_{2\,(Gas\text{-}e)}$), pH (Seawater Scale, pH_{SW})*, Carbonate Ion Concentration ($[CO_3^{2-}]$)*, Bicarbonate Ion Concentration ($[HCO_3^-]$)*, Dissolved CO_2 ($[CO_2]_{(SW)}$)*, and Calcite Saturation State (Ω_C)*] and Measured Parameters [Salinity (Sal)†, Temperature (T)†, Total Scale pH (pH_T)†, Total Alkalinity (TA)*, and Dissolved Inorganic Carbon (DIC)*] of Experimental treatments.*

		Low pCO_2	Low pCO_2 w/ crab	Mid pCO_2	Mid pCO_2 w/ crab	High pCO_2	High pCO_2 w/crab
				Calculated Parameters			
$pCO_{2\,(gas\text{-}e)}$	(ppm-v)	478	519	734	835	9,567	8,980
	SE	20	19	24	27	394	386
	Range	300–897	313–778	544–1,023	619–1,110	5,913–14,599	5,164–13,561
pH_T		8.10	8.02	7.95	7.86	6.98	6.97
	SE	0.02	0.02	0.02	0.02	0.02	0.02
	Range	7.82–8.28	7.81–8.22	7.79–8.09	7.61–8.00	6.80–7.15	6.76–7.19
$[CO_3^{2-}]$	(μM)	302	238	234	180	34	31
	SE	14	12	9	7	1	1
	Range	113–428	104–407	132–316	73–244	23–48	17–53
$[HCO_3^-]$	(μM)	2,168	1,983	2,401	2,236	3,258	3,016
	SE	38	40	27	41	20	30
	Range	1,585–2,568	1,466–2,452	2,024–2,572	1,679–2,796	2,866–3,434	2,747–3,366
$[CO_2]_{(SW)}$	(μM)	13	14	21	23	268	256
	SE	1	1	1	1	10	11
	Range	8–25	9–21	16–29	17–32	166–396	145–378
Ω_C		7.3	5.7	5.6	4.3	0.7	0.6
	SE	0.3	0.3	0.2	0.2	0.0	0.0
	Range	2.6–10.4	2.4–9.9	3.1–7.6	1.7–5.8	0.5–1.1	0.3–1.1
				Measured Parameters			
Salinity		31.8	31.8	31.7	31.6	31.8	31.8
	SE	0.04	0.04	0.04	0.11	0.04	0.05
	Range	30.5–33.0	30.5–32.6	30.5–32.5	21.7–33.2	30.7–32.8	30.7–33.3
T	(°C)	25.7	26.4	25.4	25.8	26.2	25.4
	SE	0.1	0.1	0.1	0.1	0.1	0.1
	Range	24.2–28.8	24.4–30.4	24.4–28.3	23.5–29.8	23.2–30.5	24.4–28.4
pH_T		8.15	8.01	7.97	7.87	6.96	6.91
	SE	0.01	0.01	0.01	0.01	0.01	0.01
	Range	8.09–8.54	7.92–8.35	7.96–8.25	7.79–8.22	6.84–7.98	6.90–7.22
TA	(μM)	2,865	2,542	2,940	2,657	3,335	3,086
	SE	62	60	43	53	20	31
	Range	1,865–3,195	1,731–3,248	2,342–3,199	1,861–3,333	2,960–3,517	2,801–3,450
DIC	(μM)	2,484	2,236	2,656	2,441	3,560	3,302
	SE	48	49	34	47	25	31
	Range	1,716–2,814	1,590–2,802	2,185–2,852	1,784–3,060	3,073–3,809	2,963–3,653

SE = standard error; †$n = 99$ or *$n = 33$ for each treatment.

2.2. Carbonate Conditions of Experimental Seawaters

Experimental organisms were raised in seawater with calculated pCO_2 (SE) of 499 (14), 785 (19), and 9,274 (276) μatm (Table 1), corresponding to near-modern pCO_2, predicted end-century pCO_2, and a level that exceeds the highest pCO_2 predicted to be experienced by open-ocean organisms. Although the high-pCO_2 treatment is not realistic for open-ocean seawater, such levels occur seasonally in both healthy and degraded estuaries (Cai & Wang, 1998; Ringwood & Keppler, 2002; Waldbusser et al., 2011) where oysters and mud crabs are prevalent. Furthermore, the elevated alkalinity of seawater formulated from *Instant Ocean Sea Salt* (ca. 2,500–3,300 μM experimental versus ca. 2,000–2,500 μM natural; Cai & Wang, 1998; Riebesell et al., 2010; Zeebe & Wolf-Gladrow, 2001), requires higher pCO_2 levels to approximate the pH levels and calcite saturation states that have been previously employed in related studies and to better approximate the lower seawater saturation states experienced by intertidal organisms (Bibby et al., 2007; de la Haye et al., 2011, 2012; Dissanayake et al., 2010). Although the trace elemental composition of Instant Ocean Sea Salt differs subtly from that of natural seawater, its major and minor elemental composition, as well as the total alkalinity and calcite saturation state of the resulting seawater, was the most similar to that of natural seawater when compared with eight other commercial sea salt mixes (Atkinson & Bingman, 1997). Nevertheless, small differences in seawater chemistry inevitably exist between the experimental treatments and the native waters of the oysters and mud crabs.

Partial pressures of CO_2 were established by mixing pure compressed CO_2 with compressed air using *Aalborg* digital solenoid-valve mass flow controllers, and sparging these mixed gases with microporous ceramic airstones into the experimental aquaria. The pCO_2 of the mixed gases was measured with a *Qubit S151* infrared pCO_2 analyzer calibrated with certified air-CO_2 gas standards (precision = ±2.0%; accuracy = ±1.8%). Salinity (SE) was formulated at 31.8 (0.02) with *Instant Ocean Sea Salt* and deionized water. Temperature (SE) was maintained at 25.8 (0.04) °C with 50 W electric heaters.

2.3. Measurement and Calculation of Carbonate System Parameters

Temperature, pH, and salinity were measured every 2 days, while pCO_2 of mixed gases was measured weekly (Table 1). The temperature was measured with a NIST-calibrated partial-immersion organic-filled glass thermometer (precision + 0.3%, accuracy + 0.4%). Salinity was measured with a YSI 3200 conductivity meter with a YSI 3440 cell ($K = 10$) that was calibrated with seawater certified reference material (CRM) of known salinity provided by the laboratory of Prof. A. Dickson of Scripps Institute of Oceanography. Seawater pH was measured with a Thermo Scientific Orion two Star benchtop pH meter with an Orion 9156BNWP pH probe, calibrated with 7.00 and 10.01 Orion NBS buffers traceable to NIST standard reference material and with Dickson CRMs of known pH. On a weekly basis, seawater dissolved inorganic carbon (DIC) was measured via coulometry (*UIC 5400*) and total alkalinity (TA) was measured via closed-cell potentiometric Gran titration calibrated with certified Dickson TA/DIC standards. Measurement of DIC and TA of the CRMs were consistently within 0.3% of certified values. Differences between the measured and certified TA and DIC values of the CRMs were used to correct measurements of experimental seawater solutions. Seawater pCO_2, pH, carbonate ion concentration ($[CO_3^{2-}]$), bicarbonate ion concentration ($[HCO_3^-]$), aqueous CO_2, and calcite saturation state (Ω_C) were calculated from measured DIC, TA, temperature, and salinity with the program CO_2SYS (Lewis & Wallace, 1998), using Roy et al. (1993) values for K_1 and K_2 carbonic acid constant, the Mucci (1983) value for stoichiometric aragonite solubility product, and an atmospheric pressure of 1.015 atm.

2.4. Quantification of Calcification Rates Via Buoyant Weighing

Calcification rates of oysters and crabs were estimated using an empirically calibrated buoyant weighing technique (Ries et al., 2009). Specimens were weighed at the beginning of the experiment and at 71 days. Each specimen was suspended at a depth of 10 cm by aluminum wire from a *Cole-Parmer* bottom-loading scale (precision ± 0.001; accuracy ± 0.002) in seawater of temperature and salinity consistent with that of the experimental treatments. A plastic-coated zinc mass standard was intermittently weighed to ensure consistency of the buoyant weight method.

Buoyant weight-dry $CaCO_3$ weight relationships for oysters and crabs were empirically derived by plotting final dry $CaCO_3$ weights (after removal of organic matter) against final buoyant weights of 49 oysters and 18

crabs randomly selected from the three pCO_2 (control—499 μatm, moderate—785 μatm, high—9273 μatm) treatments used in experiments. Oyster dry $CaCO_3$ weight was the dry weight (70 °C, 24 h) of the shell after mechanical removal of soft tissue. Crab dry $CaCO_3$ weight was the dry weight of the crab carapace after organic matter was removed via combustion in a muffle furnace at 500 °C for 6 h. Buoyant weight-dry $CaCO_3$ weights for specimens from all treatments were highly correlated (oyster: $R^2 = 0.9976$, $p < 0.001$; crab: $R^2 = 0.9828$, $p < 0.001$) and similar among treatments for each species, indicating that densities of crab and oyster shells did not vary appreciably among treatments (Ries et al., 2009). Thus, a single linear equation for each species was used to convert buoyant weight to dry weight to estimate net calcification rates:

Oyster: Dry weight (mg) = 1.4796 * Buoyant weight (mg) – 0.5204, SE = 0.0078;

Crab: Dry weight (mg) = 1.2306 * Buoyant weight (mg) – 0.0110, SE = 0.0407.

2.5. Scanning Electron Imaging

Secondary electron images of the oyster specimens (inner and outer shell surfaces) from each of the six treatments (two crab presence and three pCO_2 treatments) were obtained with a tungsten-filament variable pressure *Tescan Vega 3 LMU* scanning electron microscope (accelerating voltage = 20 kV) operated under high-vacuum at 8-times to 1400-times magnification. Crab presence treatments are combined in presentation of the results.

2.6. Statistics

Crab buoyant weight data contained a number of strong outliers across all acidification treatments that appear to represent a group of crabs that were in a molting phase at the start of the experiment. These crabs ($n = 8$) exhibited change in buoyant weights greater than 29% and initial shell densities below 0.032 mg buoyant weight per mm carapace width, while the remainder exhibited buoyant weight changes of 12% and initial densities greater than 0.035. These individuals were therefore excluded from further analysis.

Generalized linear mixed-effects models were used to analyze the results of this study, followed by hierarchical model selection using corrected Akaike Information Criterion (AICc). Change in oyster buoyant weight was evaluated with the variables pCO_2 (control, moderate, high), crab cue (present, absent), and their interaction as fixed factors and tank as a random factor ($n = 507$). Model evaluation for change in crab buoyant weight included pCO_2, initial carapace density (initial buoyant weight/carapace width), and their interaction as fixed factors, and tank as a random factor ($n = 51$). Following model identification, an ANOVA was run on the preferred model and Tukey's HSD post hoc tests were used to conduct pairwise mean comparisons for all levels of significant main effects and interactions. Both crab and oyster calcification datasets passed Levene's test for heteroskedasticity ($p > 0.05$). All statistical analyses were performed with JMP statistical software.

3. Results

3.1. Impact of Ocean Acidification on Oyster Calcification

Eastern oyster specimens maintained net-positive calcification rates [percent-change in buoyant weight (SE)] within all treatments [control-pCO_2: 10.936 (0.592) %; moderate-pCO_2: 10.944 (0.306) %; high-pCO_2: 9.016 (0.542) %; Figure 1a]. AICc identified the model containing only fixed effect of pCO_2, but not crab cue, as the optimal model of oyster calcification rate. ANOVA confirmed that pCO_2 treatment significantly decreased oyster calcification rate ($F_{2,504} = 7.21$, $p < 0.001$). Oyster calcification rates in the control-pCO_2 and moderate-pCO_2 treatments were significantly greater than in the high-pCO_2 treatment (Tukey's HSD, $p < 0.05$), but were not significantly different from each other (Tukey's HSD, $p > 0.05$).

Secondary electron imaging (SEI) revealed no difference across pCO_2 treatments in macrostructure of interior shells of eastern oysters (Figures 2a–2c). In contrast, exterior shells (Figures 2d–2f) and exterior shell edges (Figures 2g–2i) exhibited pronounced delamination of the periostracum in the high-pCO_2 treatment (undersaturated with respect to calcite) compared to shells produced under both control and moderate pCO_2 treatments. Secondary electron imaging of the prismatic layer of the shell exterior revealed evidence

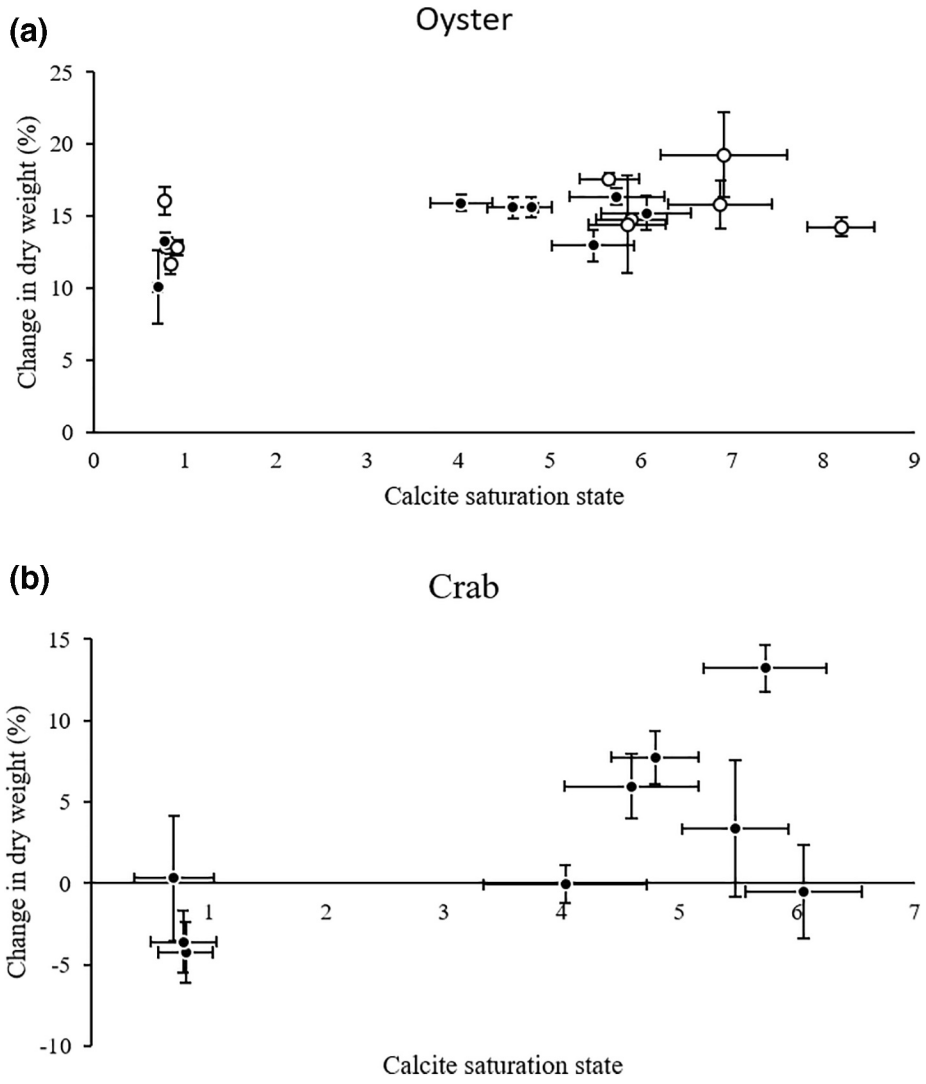

Figure 1. Mean (±SE) %-change in dry weight and mean (±SE) calcite saturation state of experimental waters for (a) eastern oyster, *C. virginica*, and (b) Atlantic mud crab, *P. herbstii*. Calcification rates of both oysters and crabs were significantly ($p < 0.05$) reduced under the highest pCO_2 treatment, but not significantly ($p > 0.05$) impacted by more moderate pCO_2 increases. Presence of crab cue (A; closed circles: oysters reared with crabs present, open circles: oysters reared without crabs present) was not included in the optimal model selected by AICc. Notably, oysters maintained net-positive calcification rates across all pCO_2 treatments. AICc, Akaike Information Criterion.

of minor dissolution in the moderate-pCO_2 treatment (Figure 2k) and more intense dissolution in the high-pCO_2 treatment (Figure 2l), contrasting the lack of visually apparent dissolution of prismatic layers of the exterior shells for oysters reared under the control pCO_2 condition (Figure 2j). The foliated units of the interior portion of oyster shells produced under the high-pCO_2 treatment (Figure 2o) were characterized by larger and thicker calcite rhombs with a more euhedral habit than the homologous crystals formed under the control-pCO_2 (Figure 2m) or moderate-pCO_2 treatments (Figure 2n), which were smaller, thinner, and more acicular in habit.

3.2. Impact of Ocean Acidification on Crab Calcification

Atlantic mud crabs were only able to maintain net-positive calcification rates [percent-change in buoyant weight (SE)] in the control-pCO_2 and moderate-pCO_2 treatments [control-pCO_2: 4.699 (1.876) %; moderate-pCO_2: 4.062 (0.984) %], and exhibited net dissolution in the high-pCO_2 treatment [−2.269 (1.133) %;

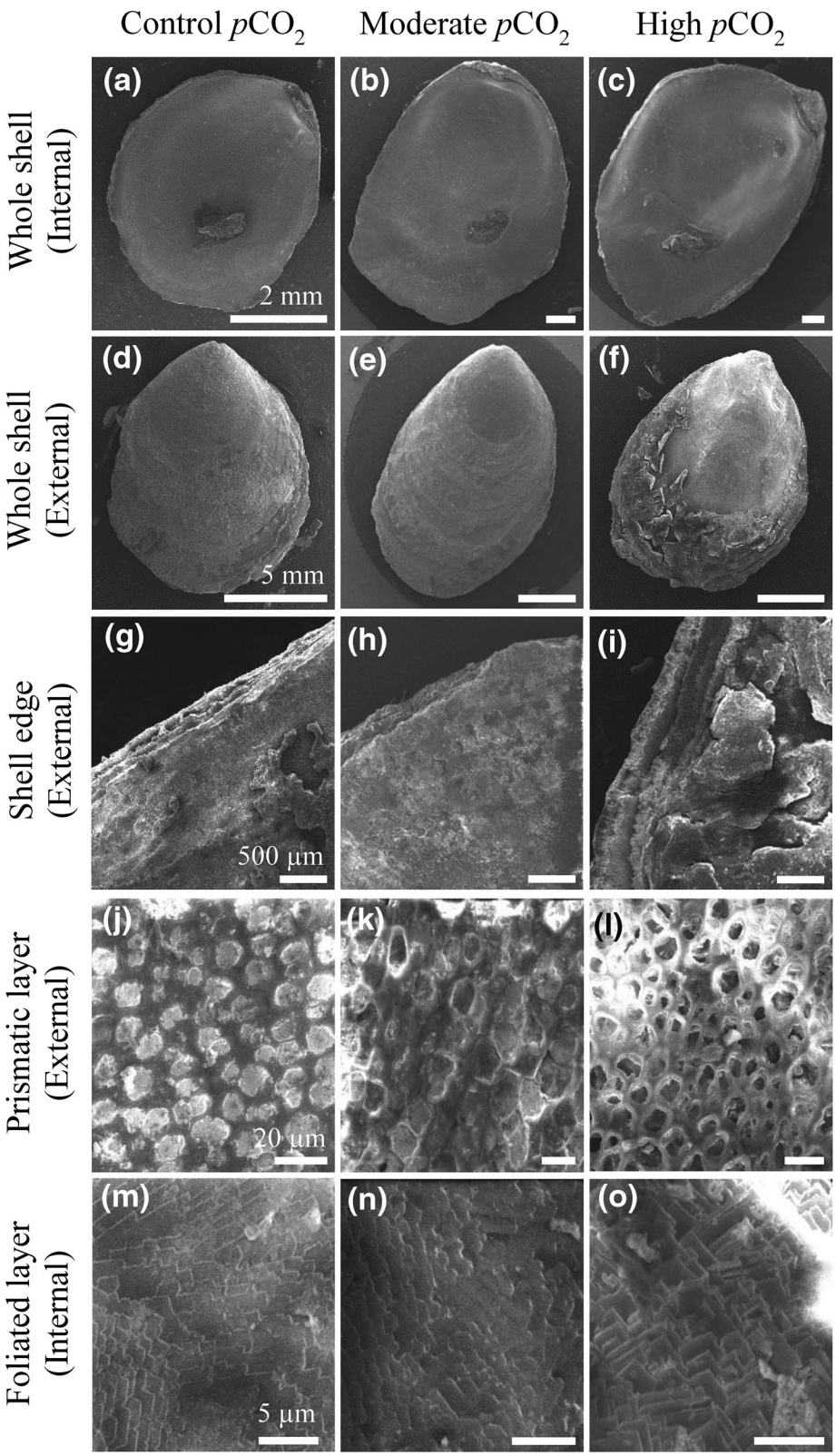

Figure 2. Secondary electron images of representative oyster shell from different pCO_2 treatments (Tungsten-filament variable pressure *Tescan Vega 3 LMU*; accelerating voltage = 20 kV; high-vacuum mode; magnification = 8 – 1,400×). Scale bars are equivalent within rows. Although changes in shell macrostructure [i.e., gross morphology of shell interior (A–C) and exterior (D–F)] are evident only in the highest pCO_2 treatment, changes in shell microstructure (i.e., exterior shell edge (G–I), exterior prismatic layer (J–L), interior foliated layer (M–O)] are discernible in both the moderate-pCO_2 and high-pCO_2 treatments.

Figure 1b]. AICc identified the model with only the fixed effect of pCO_2 as the optimal model of crab calcification rate. ANOVA confirmed that pCO_2 significantly decreased crab calcification rate ($F_{2,48} = 9.18$, $p < 0.001$). Like for the oysters, crab calcification rates in the control and moderate-pCO_2 treatments were significantly less than in the high-pCO_2 treatment (Tukey's HSD, $p < 0.05$), but were not significantly different from each other (Tukey's HSD, $p > 0.05$).

4. Discussion

4.1. Comparison of Eastern Oyster and Mud Crab Responses to Ocean Acidification

The calcification rates of both juvenile eastern oysters and adult Atlantic mud crabs were negatively impacted by the high-pCO_2 treatments. Notably, however, oysters maintained positive net calcification rates even in the highest pCO_2 treatment that was undersaturated with respect to their calcite biomineral, while mud crabs exhibited net shell dissolution under this condition. This ability of oysters to continue forming new shell in the highest pCO_2 treatment, while the mud crabs could not, may be attributable to differences in the Mg-content of their respective calcitic shells. Oysters produce their shell from low-Mg calcite (molar Mg/Ca < 0.01), which is less soluble than the high-Mg calcite (molar Mg/Ca = 0.08–0.12) shell formed by mud crabs. It is also possible that the high energetic demands of the crabs' intermittent molting style of calcification, compared with the oysters' more continuous mode of calcification, renders the crab more vulnerable to ocean acidification—although the data generated from the present study are insufficient to evaluate this hypothesis.

4.2. Comparison with Prior Work Investigating Impact of Ocean Acidification on Crab Calcification

No studies have investigated the impact of ocean acidification on mud crab calcification. However, prior investigations into the impact of ocean acidification on other species of crabs have yielded mixed outcomes. For instance, Ries et al. (2009) found that adults of three species of decapod crustacea, including the eastern king prawn (*P. plebejus*), American lobster (*H. americanus*), and blue crab (*C. sapidus*), exhibited increasing calcification rates with increasing pCO_2. In contrast, Long et al. (2013) found that calcification rates of juvenile Tanner crabs (*C. bairdi*) decreased under elevated pCO_2, while calcification rates of the juvenile red king crab (*P. camtschaticus*) were not affected by increasing pCO_2. The negative response to increasing pCO_2 exhibited by the mud crabs in the present study is consistent with the response of juvenile tanner crabs, but contrasts the more resilient responses of American lobsters, eastern King prawns, blue crabs, and Tanner crabs.

The differences in these species' responses to CO_2-induced ocean acidification may arise from differences in ability regulate pH at their sites of calcification, differences in the Mg-content (and thus solubility) of their calcitic carapaces (Ries, 2011), differences in the efficacy of the their epicuticle in isolating their carapace from the external seawater (Ries et al., 2009), and differences in the duration and/or degree of experimental exposure (Pane & Barry, 2007; Small et al., 2010; Spicer et al., 2006). Future studies aimed at partitioning the relative importance of these potential mechanisms in conferring resilience (or vulnerability) to ocean acidification will improve our understanding of calcification within decapod crustacea and inform predictions of their response to future ocean acidification.

4.3. Comparison with Prior Work Investigating Impact of Ocean Acidification on Oyster Calcification

Previous studies investigating oysters' calcification response to ocean acidification have either found no change in net calcification rates (Dickinson et al., 2012) or decreasing net calcification rates with increasing pCO_2 across a wide range of life stages (Beniash et al., 2010; Downey-Wall et al., 2020; Gazeau et al., 2007; Miller et al., 2009; Ries et al., 2009). Oyster larvae utilize the aragonite polymorph of $CaCO_3$ in shell development and are therefore considered more vulnerable to ocean acidification than juveniles or adults that utilize the less soluble calcite polymorph. The shell mass of D-stage Eastern oyster larvae reared for 28 days in seawater Ω_A ranging from 1.2 to 0.6 decreased linearly with declining Ω_A (Miller et al., 2009). However,

the shell mass of larval Suminoe oysters (*Crassostrea ariakensis*) investigated in the same experiment did not vary with Ω_A and maintained positive net calcification rates across all treatments, including those undersaturated with respect to the larvae's aragonite shell mineral ($\Omega_A < 1$). Postmetamorphosis oysters switch to utilizing predominantly calcite for shell construction. Three-week postmetamorphosis eastern oyster spat subjected to Ω_C of 8.4 and 1.4 had reduced shell growth in the lower Ω_C treatment (Beniash et al., 2010). Short-term exposure of Pacific oyster spat to decreasing Ω_C (5.7-2.0) yielded similar linear decreases in net calcification rates (Gazeau et al., 2007). Likewise, the net calcification rate of adult eastern oysters declined linearly when exposed for 60 days to Ω_C ranging from 4.0 to 1.1 (Ries et al., 2009) and in a nonlinear, threshold manner when exposed for 80 days to Ω_C ranging from 3.0 to 0.9 (Downey-Wall et al., 2020). Juvenile eastern oysters investigated in the present study exhibit a nonlinear threshold response to decreasing Ω_C (7.3-0.6), consistent with work by Downey et al. (2020) on adult eastern oysters, but contrasting the linear declines in calcification rate of adult eastern oysters observed by Gazeau et al. (2007) and Ries et al. (2009). Dickinson et al. (2012) found no significant differences in net calcification rate of adult eastern oysters across a wide range of Ω_C (9.1-1.6), although they attribute the lack of statistical significance in part to high variance in calcification rates among replicate individuals within experimental treatments. These results, combined with the relatively high within-treatment variance observed in the present study, suggest that there is a high degree of variability in the response of individual eastern oysters to reduced Ω_C. Determining whether there is a genetic basis for this variability in calcification response to ocean acidification warrants further investigation.

4.4. Impact of Ocean Acidification on Oyster Shell Microstructure

Secondary electron imaging of the oyster shells revealed significant dissolution of the shell exterior and resulting delamination and degradation of the periostracum in the highest pCO_2 treatment (Figures 2g–2l), despite the oyster's continued production of new shell material that was sufficient to maintain net-positive calcification rates in calcite-undersaturated conditions. The observation that the exterior portion of the oyster shell dissolved under the highest pCO_2 treatment underscores the threat that ocean acidification poses for bivalves like oysters, while the oyster's ability to maintain net-positive rates of calcification under these conditions (Figure 2a) reveals the strong physiological control that they exhibit over their shell-building process.

The combination of secondary electron imaging from this study with prior work on the dissolution kinetics of oyster shell calcite (Ries et al., 2016) suggests that the observed differences in oyster calcification rate among the various pCO_2 treatments is at least partly attributable to the dissolution of exterior shell in the high-pCO_2 (i.e., calcite-undersaturated) treatment. Nevertheless, the oysters were able to maintain net-positive rates of calcification in seawaters that were highly undersaturated with respect to their calcite mineral by maintaining rates of gross calcification (on shell interior) that exceeded rates of gross dissolution (on shell exterior).

Recent studies have shown that the pH of the calcifying extrapallial fluid of eastern oysters is less than seawater pH under control (i.e., ambient) pCO_2 conditions (Crenshaw, 1972; Sutton et al., 2018), but increases relative to seawater pH with increasing pCO_2 (Downey-Wall et al., 2020; Liu et al., 2020)—suggesting that oysters regulate extrapallial fluid pH to mitigate the impacts of ocean acidification on shell formation. However, the onset of differences in microstructure of the interior portions of the oyster shells (i.e., the actively growing portion of shell adjacent to the extrapallial fluid and mantle), combined with significantly reduced net calcification rates in the highest pCO_2 treatment, suggest that the oysters' regulation of extrapallial fluid pH is insufficient to completely mitigate the impacts of ocean acidification on juvenile oyster calcification.

Secondary electron images of the prismatic layer also revealed intact organic matrices (e.g., periostracum) under all pCO_2 treatments, similar to what has been observed for other bivalves exposed to high-pCO_2 conditions (Green et al., 2004; Welladsen et al., 2010). However, in contrast to Welladsen's (2010) observation that the periostracum of the Akoya pearl oyster (*Pinctada fucata*) was not impacted by high-pCO_2 conditions, the periostracum of the juvenile oysters cultured in the high-pCO_2 treatment of the present study was absent from more than half of each shell's external surface area, and was heavily degraded where it remained (Figures 2f and 2i). It appears that the undersaturated seawater ($\Omega_C < 1$) in the highest-pCO_2 treatment dissolved away shell material directly beneath the periostracum, causing the periostracum to

delaminate from the shell surface, thereby exposing more of the unprotected shell to dissolution. It is possible that a positive feedback exists between these two processes, by which exterior shell dissolution causes delamination of the periostracum, thereby yielding further shell dissolution. Thus, net calcification rates toward the end of the experiment—when more of the periostracum was missing—may be higher than reflected by the net calcification rates determined across the entire duration of the experiment.

4.5. Impact of Crab Cue on Oyster Calcification Rate

As previously noted, the present study was conducted as part of a set of experiments designed to investigate the impact of ocean acidification on various aspects of the juvenile oyster-mud crab model predator-prey system. As such, the larger study included treatments to test for the effect of predator cues on prey defenses (e.g., oyster calcification rate; Newell et al., 2007). However, a number of methodological choices—some made in order not to bias the behavioral components of the study (Dodd et al., 2015) and others made without the benefit of forthcoming research (present study conducted in 2011; Johnson & Smee, 2012; Robinson et al., 2014)--severely limited the likelihood of observing a change in oyster calcification in response to a predator cue.

Specifically, Johnson and Smee (2012) found that eastern oysters in the Gulf of Mexico larger than ~10 mm did not exhibit differences in shell growth when exposed to *P. herbstii* under normal (i.e., control) conditions. The oyster used in the present study were larger than this threshold (18.7 ± 3.8 mm shell height) and therefore may not exhibit an increased calcification in response to crab presence. Although Robinson et al. (2014) reported that the presence of *P. herbstii* induced a defense response in eastern oysters, the response of smaller oysters (2–5 mm) to *P. herbstii* was approximately 50% less than their response to the co-occurring predatory crab *C. sapidus* (Robinson et al., 2014). Furthermore, mud crabs were fed brine shrimp in the present study to avoid biasing the crabs' perception of oysters as a food source (Dodd et al., 2015), which may have reduced the strength of the crab cue as prey have been shown to respond more strongly to predators that have feed on conspecifics (Griffiths & Richardson, 2006; Hill & Weissburg, 2014). These factors may have reduced the likelihood of identifying an effect of mud crab presence on juvenile oyster calcification under conditions of ocean acidification. This line of inquiry requires further investigation.

5. Conclusion

The present study revealed that the calcification rates of two estuarine calcifiers involved in a classic predator-prey model, adult mud crabs, and juvenile eastern oysters, exhibited negative responses to CO_2-induced ocean acidification. However, the magnitudes of their responses differed, with oysters exhibiting net-positive calcification and mud crabs net dissolution in the highest pCO_2 treatment that was undersaturated with respect to calcite. These disparate responses to ocean acidification, combined with prior work showing that the foraging behavior of mud crabs on juvenile oysters is impaired by ocean acidification (Dodd et al., 2015), provides empirical support for the assertion that future ocean acidification will alter the relationship between the species in this classical predator-prey model system.

Secondary electron imaging of the oyster shells revealed significant dissolution of the shell exterior and resulting delamination and degradation of the periostracum in the highest pCO_2 treatment, despite the oyster's continued production of new shell material that was sufficient to maintain net-positive calcification rates even in calcite-undersaturated conditions. The observation that the exterior portion of the oyster shell dissolved under the highest pCO_2 treatment underscores the threat that ocean acidification poses for bivalves like oysters, while the oyster's ability to maintain net-positive rates of calcification under these conditions reveals the strong physiological control that they exhibit over their shell-building process.

The nonlethal but still deleterious effects of ocean acidification on calcification rates of these two species may increase their energetic costs of calcification, as well as their vulnerability to disease, warming, predation, pollution, overharvesting, sea level rise, and other environmental stressors (Doney et al., 2009, 2012, references therein). Availability of oyster reef habitat may also decline as acidification displaces populations from lower salinity waters (with correspondingly lower calcite saturation states) where oyster reefs are typically established due to decreased disease and predation (Aronhime, 2010; Haskin & Ford, 1982; Paynter & Burreson, 1991). Although we have only begun to assess the extent to which ocean acidification will impact

marine organisms, these results support the mounting evidence that effects will be variable and complex, and could manifest over scales ranging from individual mineral grains to entire ecosystems.

Data Availability Statement

Data are available at: http://www.bco-dmo.org/project/2152.

Acknowledgments
We thank Karl Castillo, Travis Courtney, and Cassandre Lazar for their assistance in implementing the experiment. We also thank two anonymous reviewers for their constructive feedback. The authors declare that the research was conducted in the absence of any commercial or financial relationships that could be construed as a potential conflict of interest.
L. F. Dodd, J. H. Grabowski, Justin B. Ries, and M. F. Piehler designed the experiments. L. F. Dodd maintained the experiment and analyzed calcification, stress-strain, and SEI data. I. Westfield performed water chemistry analyses and Justin B. Ries analyzed water chemistry data and obtained electron images of oyster shells. L.D. and Justin B. Ries wrote early drafts of the manuscript and all authors contributed substantially to revisions.
NSF-BIO-OCE 1357665 (to Justin B. Ries), MIT SeaGrant/NOAA NA14OAR41705710004054 (to Justin B. Ries), NOAA NA14NMF4540072 (to Justin B. Ries and J. H. Grabowski), NSF-BIO-OCE 0961929 (to M. F. Piehler).

References

Aronhime, B. R. (2010). *Predator-prey interaction in estuarine bivalves: Size selection, effects of salinity, and indirect interactions (LSU Doctoral dissertations 3517)*. Baton Rouge, LA: Louisiana State University. Retrieved from https://digitalcommons.lsu.edu/gradschool_dissertations/3517

Atkinson, M., & Bingman, C. (1997). Elemental composition of commercial seasalts. *Journal of Aquaculture and Aquatic Sciences, 8*, 39–43.

Azevedo, L. B., De Schryver, A. M., Hendriks, A. J., & Huijbregts, M. A. J. (2015). Calcifying species sensitivity distributions for ocean acidification. *Environmental Science & Technology*, *49*, 1495–1500. https://doi.org/10.1021/es505485m

Beniash, E., Ivanina, A., Lieb, N. S., Kurochkin, I., & Sokolova, I. M. (2010). Elevated level of carbon dioxide affects metabolism and shell formation in oysters *Crassostrea virginica*. *Marine Ecology Progress Series*, *419*, 95–108. https://doi.org/10.3354/meps08841

Bibby, R., Cleall-Harding, P., Rundle, S., Widdicombe, S., & Spicer, J. (2007). Ocean acidification disrupts induced defences in the intertidal gastropod *Littorina littorea*. *Biology Letters*, *3*, 699–701. https://doi.org/10.1098/rsbl.2007.0457

Brewer, P. G. (1997). Ocean chemistry of the fossil fuel CO_2 signal: The haline signal of 'business as usual'. *Geophysical Research Letters*, *24*, 1367–1369. https://doi.org/10.1029/97GL01179

Cai, W.-J., & Wang, Y. (1998). The chemistry, fluxes, and sources of carbon dioxide in the estuarine waters of the Satilla and Altamaha Rivers, Georgia. *Limnology & Oceanography*, *43*, 657–668. https://doi.org/10.4319/lo.1998.43.4.0657

Cameron, J. N. (1989). Post-molt calcification in the blue crab, *Callinectes sapidus*: Timing and mechanism. *Journal of Experimental Biology*, *143*, 285–304.

Carriker, M. R., Swann, C. P., Prezant, R. S., & Counts, C. L., III (1991). Chemical elements in the aragonitic and calcitic microstructural groups of shell of the oyster *Crassostrea virginica*: A proton probe study. *Marine Biology*, *109*, 287–297.

Chave, K. E. (1954). Aspects of the biogeochemistry of magnesium. 1: Calcareous marine organisms. *The Journal of Geology*, *62*, 266–283.

Crenshaw, M. A. (1972). The inorganic composition of molluscan extrapallial fluid. *The Biological Bulletin*, *143*, 506–512. https://doi.org/10.2307/1540180

Crenshaw, M. A., & Neff, J. M. (1969). Decalcification at the mantle-shell interface in molluscs. *American Zoologist*, *9*, 881–885. https://doi.org/10.1093/icb/9.3.881

de la Haye, K. L., Spicer, J. I., Widdicombe, S., & Briffa, M. (2011). Reduced sea water pH disrupts resource assessment and decision making in the hermit crab *Pagurus bernhardus*. *Animal Behaviour*, *82*, 495–501. https://doi.org/10.1016/j.anbehav.2011.05.030

de la Haye, K. L., Spicer, J. I., Widdicombe, S., & Briffa, M. (2012). Reduced pH sea water disrupts chemo-responsive behavior in an intertidal crustacean. *Journal of Experimental Marine Biology and Ecology*, *412*, 134–140. https://doi.org/10.1016/j.jembe.2011.11.013

Dickinson, G. H., Ivanina, A. V., Matoo, O. B., Pörtner, H. O., Lannig, G., Bock, C., et al. (2012). Interactive effects of salinity and elevated CO_2 levels on juvenile eastern oysters, *Crassostrea virginica*. *Journal of Experimental Biology*, *215*, 29–43. https://doi.org/10.1242/jeb.061481

Dissanayake, A., Clough, R., Spicer, J. I., & Jones, M. B. (2010). Effects of hypercapnia on acid-base balance and osmo-/iono-regulation in prawns (Decapoda: Palaemonidae). *Aquatic Biology*, *11*, 27–36. https://doi.org/10.3354/AB00285

Dodd, L. F., Grabowski, J. H., Piehler, M. F., Westfield, I., & Ries, J. B. (2015). Ocean acidification impairs crab foraging behavior. Proceedings of the Royal Society B: Biological Sciences, 282, 20150333. https://doi.org/10.1098/rspb.2015.0333

Doney, S. C., Fabry, V. J., Feely, R. A., & Kleypas, J. A. (2009). Ocean acidification: The other CO_2 problem. *Annual Review of Marine Science*, *1*, 169–192. https://doi.org/10.1146/annurev.marine.010908.163834

Doney, S. C., Ruckelshaus, M., Duffy, J. E., Barry, J. P., Chan, F., English, C. A., et al. (2012). Climate change impacts on marine ecosystems. *Annual Review of Marine Science*, *4*, 11–37. https://doi.org/10.1146/annurev-marine-041911-111611

Downey-Wall, A. M., Cameron, L. P., Ford, B. M., McNally, E. M., Venkataraman, Y. R., Roberts, S. B., et al. (2020). Ocean acidification induces subtle shifts in gene expression and DNA methylation in mantle tissue of the Eastern oyster (*Crassostrea virginica*). *Frontiers in Marine Science*, *7*, 566419. https://doi.org/10.3389/fmars.2020.566419

Espinosa, E. P., & Allam, B. (2006). Comparative growth and survival of juvenile hard clams, *Mercenaria mercenaria*, fed commercially available diets. *Zoo Biology*, *25*, 513–525. http://doi.org/10.1002/zoo.20113

Fabry, V. J., McClintock, J. B., Mathis, J. T., & Grebmeier, J. M. (2009). Ocean acidification at high latitudes: The bellwether. *Oceanography*, *22*, 160–171. https://doi.org/10.5670/oceanog.2009.105

Gattuso, J.-P., Frankignoulle, M., Bourge, I., Romaine, S., & Buddemeier, R. W. (1998). Effect of calcium carbonate saturation of seawater on coral calcification. *Global and Planetary Change*, *18*, 37–46. https://doi.org/10.1016/S0921-8181(98)00035-6

Gazeau, F., Quiblier, C., Jansen, J. M., Gattuso, J.-P., Middelburg, J. J., & Heip, C. H. R. (2007). Impact of elevated CO_2 on shellfish calcification. *Geophysical Research Letters*, *34*, L07603. https://doi.org/10.1029/2006GL028554

Ginger, K. W. K., Vera, C. B. S., Dineshram, R., Dennis, C. K. S., Adela, L. J., Ziniu, , Y., & Thiyagarajan, V.. (2013). Larval and post-larval stages of Pacific oyster (*Crassostrea gigas*) are resistant to elevated CO_2. *PloS One*, *8*(5), e64147. https://doi.org/10.1371/journal.pone.0064147

Green, M. A., Jones, M. E., Boudreau, C. L., Moore, R. L., & Westman, B. A. (2004). Dissolution mortality of juvenile bivalves in coastal marine deposits. *Limnology & Oceanography*, *49*, 727–734. https://doi.org/10.4319/lo.2004.49.3.0727

Griffiths, C. L., & Richardson, C. A. (2006). Chemically induced predator avoidance behavior in the burrowing bivalve *Macoma balthica*. *Journal of Experimental Marine Biology & Ecology*, *331*(1), 91–98. http://doi.org/10.1016/j.jembe.2005.10.002

Harvey, B. P., Gwynn-Jones, D., & Moore, P. J. (2013). Meta-analysis reveals complex marine biological responses to the interactive effects of ocean acidification and warming. *Ecology and Evolution*, *3*, 1016–1030. https://doi.org/10.1002/ece3.728

Haskin, H. H., & Ford, S. E. (1982). *Haplosporidium nelsoni* (MSX) on Delaware Bay seed oyster beds: A host-parasite relationship along a salinity gradient. *Journal of Invertebrate Pathology*, *40*, 388–405. https://doi.org/10.1016/0022-2011(82)90178-1

Hendriks, I. E., Duarte, C. M., & Álvarez, M. (2010). Vulnerability of marine biodiversity to ocean acidification: A meta-analysis. *Estuarine, Coastal and Shelf Science*, *86*, 157–164. https://doi.org/10.1016/j.ecss.2009.11.022

Hill, J. M., & Weissburg, M. J. (2014). Crabs interpret the threat of predator body size and biomass via cue concentration and diet. *Animal Behaviour*, *92*, 117–123. http://doi.org/10.1016/j.anbehav.2014.03.025

Hoegh-Guldberg, O., Cai, R. S., Poloczanska, E. S., Brewer, P. G., Fabry, V. J., Hilmi, K., et al. (2014). Climate change 2014: Impacts, adaptation, and vulnerability. Part B: Regional aspects. InC. B. Field, V. R. Barrows, D. J. Dokken, K. J. Mach, M. D. Mastrandrea, & T. E. Billir (Eds.), *Contribution of working group II to the Fifth Assessment Report of the Intergovernmental Panel on Climate change* (pp. 1655–1731). New York: Cambridge University Press.

Johnson, K. D., & Smee, D. L. (2012). Size matters for risk assessment and resource allocation in bivalves. *Marine Ecology Progress Series*, *462*, 103–110. http://doi.org/10.3354/meps09804

Korringa, P. (1951). On the nature and function of 'chalky' deposits in the shell of *Ostrea edulis* Linnaeus. *Proceedings of the California Academy of Sciences*, *27*, 133–158.

Kroeker, K. J., Kordas, R. L., Crim, R. N., & Singh, G. G. (2010). Meta-analysis reveals negative yet variable effects of ocean acidification on marine organisms. *Ecology Letters*, *13*, 1419–1434. https://doi.org/10.1111/j.1461-0248.2010.01518.x

Langdon, C. (2005). Effect of elevated pCO_2 on photosynthesis and calcification of corals and interactions with seasonal change in temperature/irradiance and nutrient enrichment. *Journal of Geophysical Research*, *110*, C09S07. https://doi.org/10.1029/2004JC002576

Langdon, C., Takahashi, T., Sweeney, C., Chipman, D., Goddard, J., Marubini, F., et al. (2000). Effect of calcium carbonate saturation state on the calcification rate of an experimental coral reef. *Global Biogeochemical Cycles*, *14*, 639–654. https://doi.org/10.1029/1999GB001195

Lewis and Wallace (1998). *CO2SYS: Program developed for CO_2 system calculations* (ORNL/CDIAC-105). Oak Ridge, TN: Oak Ridge National Laboratory, U.S. Department of Energy.

Liu, Y. -W., Sutton, J. N., Ries, J. B., & Eagle, R. A. (2020). Regulation of calcification site pH is a polyphyletic but not always governing response to ocean acidification. *Science Advances*, *6*(5), eaax1314. https://doi.org/10.1126/sciadv.aax1314

Long, W. C., Swiney, K. M., Harris, C., Page, H. N., & Foy, R. J. (2013). Effects of ocean acidification on juvenile red king crab (*Paralithodes camtschaticus*) and Tanner crab (*Chionoecetes bairdi*) growth, condition, calcification, and survival. *PloS One*, *8*, e60959.. https://doi.org/10.1371/journal.pone.0060959

MacDonald, J., Freer, A., & Cusack, M. (2010). Alignment of crystallographic *c*-Axis throughout the four distinct microstructural layers of the oyster *Crassostrea gigas*. *Crystal Growth & Design*, *10*, 1243–1246. https://doi.org/10.1021/cg901263p

Matoo, O. B., Ivanina, A. V., Ullstad, C., Beniash, E., & Sokolova, I. M. (2013). Interactive effects of elevated temperature and CO_2 levels on metabolism and oxidative stress in two common marine bivalves (*Crassostrea virginica* and *Mercenaria mercenaria*). *Comparative Biochemistry and Physiological Part A*, *164*, 545–553. https://doi.org/10.1016/j.cbpa.2012.12.025

Menzel, R. W., & Nichy, F. E. (1958). Studies of the distribution and feeding habits of some oyster predators in Alligator Habor, Florida. *Bulletin of Marine Science*, *8*, 125–145.

Meyer, D. L. (1994). Habitat partitioning between the xanthid crabs *Panopeus herbstii* and *Eurypanopeus depressus* on intertidal oyster reefs (*Crassostrea virginica*) in southeastern North Carolina. *Estuaries*, *17*, 674–679 https://doi.org/10.2307/1352415

Miller, A. W., Reynolds, A. C., Sobrino, C., & Riedel, G. F. (2009). Shellfish face uncertain future in high CO_2 world: Influence of acidification on oyster larvae calcification and growth in estuaries. *PloS One*, *4*, e5661. https://doi.org/10.1371/journal.pone.0005661

Mucci, A. (1983). The solubility of calcite and aragonite in sea water at various salinities, temperatures, and one atmospheric total pressure. *American Journal of Science*, *283*, 780–799. https://doi.org/10.2475/ajs.283.7.780

Newell, R. I. E., Kennedy, V. S., & Shaw, K. S. (2007). Comparative vulnerability to predators, and induced defense responses, of eastern oysters *Crassostrea virginica* and non-native *Crassostrea ariakensis* oysters in Chesapeake Bay. *Marine Biology*, *152*, 449–460.

Pane, E. F., & Barry, J. P. (2007). Extracellular acid-base regulation during short-term hypercapnia is effective in a shallow-water crab, but ineffective in a deep-sea crab. *Marine Ecology Progress Series*, *334*, 1–9. https://doi.org/10.3354/meps334001

Parker, L. M., Ross, P. M., & O'Connor, W. A. (2010). Comparing the effect of elevated pCO_2 and temperature on the fertilization and early development of two species of oysters. *Marine Biology*, *157*, 2435–2452. https://doi.org/10.1007/s00227-010-1508-3

Paynter, K. T., & Burreson, E. M. (1991). Effects of *Perkinsus marinus* infection in the eastern oyster, *Crassostrea virginica*: II. Disease development and impact on growth rate at different salinities. *Journal of Shellfish Research*, *10*, 425–431.

Plotnick, R. E., Baumiller, T., & Wetmore, K. L. (1988). Fossilization potential of the mud crab, *Panopeus* (brachyura: Xanthidae) and temporal variability in crustacean taphonomy. *Palaeogeography, Palaeoclimatology, Palaeoecology*, *63*, 27–43. https://doi.org/10.1016/0031-0182(88)90089-2

Riebesell, U., Fabry, V. J., Hansson, L., & Gattuso, J.-P. (2010). *Epoca: Guide to best Practices for ocean acidification research and data reporting*. Luxembourg: Publications Office of the European Union.

Ries, J. B. (2011). Skeletal mineralogy in a high-CO_2 world. *Journal of Experimental Marine Biology and Ecology*, *403*, 54–64. https://doi.org/10.1016/j.jembe.2011.04.006

Ries, J. B., Cohen, A. L., & McCorkle, D. C. (2009). Marine calcifiers exhibit mixed responses to CO_2-induced ocean acidification. *Geology*, *37*, 1131–1134. https://doi.org/10.1130/G30210A.1

Ries, J. B., Ghazaleh, M. N., Connolly, B., Westfield, I., & Castillo, K. D. (2016). Impacts of seawater saturation state ($\Omega A = 0.4–4.6$) and temperature (10, 25 °C) on the dissolution kinetics of whole-shell biogenic carbonates. *Geochimica et Cosmochimica Acta*, *192*, 318–337. https://doi.org/10.1016/j.gca.2016.07.001

Rindone, R. R., & Eggleston, D. B. (2011). Predator–prey dynamics between recently established stone crabs (*Menippe* spp.) and oyster prey (*Crassostrea virginica*). *Journal of Experimental Marine Biology & Ecology*, *407*, 216–225. https://doi.org/10.1016/j.jembe.2011.06.018

Ringwood, A. H., & Keppler, C. J. (2002). Water quality variation and clam growth: is pH really a non-issue in estuaries?. *Estuaries*, *25*, 901–907. https://doi.org/10.1242/jeb.082909

Robinson, E. M., Lunt, J., Marshall, C. D., & Smee, D. L. (2014). Eastern oysters *Crassostrea virginica* deter crab predators by altering their morphology in response to crab cues. *Aquatic Biology*, *20*, 111–118. http://doi.org/10.3354/ab00549

Roy, R. N., Vogel, K. M., Porter-Moore, C., Pearson, T., Good, C. E., Millero, F. J., et al. (1993). The dissociation constants of carbonic acid in seawater at salinities 5 to 45 and temperatures 0 to 45°C. *Marine Chemistry*, *44*, 249–267. https://doi.org/10.1016/0304-4203(93)90207-5

Small, D., Calosi, P., White, D., Spicer, J. I., & Widdicombe, S. (2010). Impact of medium-term exposure to CO_2 enriched seawater on the physiological functions of the velvet swimming crab *Necora puber*. *Aquatic Biology*, *10*, 11–21. https://doi.org/10.3354/ab00266

Spicer, J. I., Raffo, A., & Widdicombe, S. (2006). Influence of CO_2-related seawater acidification on extracellular acid-base balance in the velvet swimming crab *Necora puber*. *Marine Biology*, *151*, 1117–1125. https://doi.org/10.1007/S00227-006-0551-6

Sutton, J. N., Liu, Y.-W., Ries, J. B., Guillermic, M., Ponzevera, E., & Eagle, R. A. (2018). δ11B as monitor of calcification site pH in divergent marine calcifying organisms. *Biogeosciences*, *15*, 1447–1467. https://doi.org/10.5194/bg-15-1447-2018

Taylor, J. D., & Layman, M. (1972). The mechanical properties of bivalve (Mollusca) shell structure. *Paleontology*, *15*, 73–87.

Waldbusser, G. G., Voigt, E. P., Bergschneider, H., Green, M. A., & Newell, R. I. E. (2011). Biocalcification in the eastern oyster (*Crassostrea virginica*) in relation to long-term trends in Chesapeake Bay pH. *Estuaries and Coasts*, *34*, 221–231. https://doi.org/10.1007/S12237-010-9307-0

Welladsen, H. M., Southgate, P. C., & Heimann, K. (2010). The effects of exposure to near-future levels of ocean acidification on shell characteristics of *Pinctada fucata* (Bivalvia: Pteriidae). *Molluscan Research*, *30*, 125–130.

Zeebe, R. E., & Wolf-Gladrow, D. (2001). CO_2 in seawater: equilibrium, kinetics, isotopes. *Oceanography Series*, *65*, 1–341.